S. Afr. J. Chem., 2026, 80, S24–S36
https://journals.co.za/content/journal/chem/

Interaction Study of [Choline Chloride] [Formic acid] (1:6) Deep Eutectic Solvent with Alcohol and Water: Thermodynamic, Correlation and Modelling

Sibusiso Msimanga[1], Ncomeka Mgxadeni[1], Ariel Hernández[2], Indra Bahadur[1,*], Shailendra Kumar Singh[3], Faruq Mohammad[4], Sangeeta Singh[5], Kaniki Tumba[5], Ahmed Abdullah Soleiman[6]

[1]*Department of Chemistry, North-West University (Mafikeng Campus), Mmabatho, South Africa*
[2]*Facultad de Ingeniería y Negocios, Universidad de Las Américas, Concepción, Chile*
[3]*Department of Chemistry, Hansraj College, University of Delhi, Delhi, India*
[4]*Surfactants Research Chair, Department of Chemistry, College of Science, King Saud University, Riyadh, Kingdom of Saudi Arabia*
[5]*Thermodynamics-Materials-Separations Research Group, Department of Chemical Engineering, Mangosuthu University of Technology, uMlazi, Durban, South Africa*
[6]*Department of Chemistry, Southern University and A&M College, Baton Rouge, Louisiana, USA*

ABSTRACT

In recent years, deep eutectic solvents (DESs) have gained prominence as environmentally friendly and sustainable alternatives in various scientific and industrial applications. This study focuses on choline-based DES, known for its low toxicity, tunable characteristics, and diverse applications. The research delves into thermophysical properties (density (ρ) and speed of sound (u)) to analyze potential interactions between components. Binary system [Choline Chloride] [Formic acid] ([ChCl][FA])$_{(1:6)}$ with methanol, ethanol, and water was examined at T = (298.15 to 313.15 K). Excess/derived properties were investigated to provide valuable information for potential industrial-scale applications. The Redlich-Kister smoothing polynomial was employed to represent excess molar volumes and variance in isentropic compressibilities. For modeling of properties studied in this work, the Perturbed Chain Statistical Associating Fluid Theory (PC-SAFT), Nomoto's relation (NR), and Schaaff's collision theory (SCFT) were used. The PC-SAFT EoS was used to model binary mixture densities, while NR and SCFT were used to estimate the u. The PC-SAFT equation of state accurately estimated the ρ of binary mixtures, with an overall deviation of 0.16%. Additionally, when utilized to estimate the u, both methods performed well in accurately depicting the u for the mixtures, with overall deviations of 1.69% and 1.23% for SCFT and NR, respectively.

KEYWORDS

DESs, Thermophysical Properties, NR and SCFT, Schaaff's collision theory, Nomoto's relation, PC-SAFT EoS

Received 3 March 2025, revised 9 December 2025, accepted 15 January 2026

INTRODUCTION

In contemporary times, safeguarding the environment against industrial pollution is a fundamental requirement for all sectors, with a particular emphasis on the chemical industry. A crucial responsibility for chemists and chemical engineers is the development of industrial processes to foster greater sustainability.[1] It may entail either transforming processes into more sustainable states or completely substituting harmful conventional compounds for environmentally friendly alternatives. Development of substituent green solvents with less toxic characteristics has advanced significantly in recent decades. Supercritical fluids like CO_2, bio-solvents made from biomass like liquid polymers, switchable and gas-expanded solvents, glycerol, and specially designed solvents like ionic liquids (ILs) and DESs are the available possibilities.[2-4] Among these, DESs were first described as a promising class of green solvents by Abbott and coworkers in 2003 and deserve particular attention for their potential in various processes.[5]

DESs are a blend of a minimum of two compounds: one acting as the hydrogen bond donor (HBD), providing hydrogen bonds in the mixture, and another serving as the hydrogen bond acceptor (HBA), which accepts hydrogen bonds.[6,7] This balanced combination results in a mixture with a low melting point compared to the initial melting point of each component. DESs have emerged as environmentally friendly and sustainable solvents, offering distinctive properties and applications. The applications of DES are still at laboratory/pilot scale (TRLs 3-5), with promising results but early-stage of demonstrations. Metal recovery and extraction processes have advanced even further, with several pilot studies and semi-industrial demonstrations reported (TRLs 5-6). In the pharmaceutical and cosmetic fields, DESs are being investigated as excipients and formulation media, with some pre-commercial applications under evaluation (TRLs 6-7). However, large-scale industrial adoption (TRLs 9-10) is still limited, reflecting the need for further scale-up and validation.[8-10]

Thermodynamic studies explore the principles and laws governing energy and its transformations in physical systems. These studies encompass various branches, classical thermodynamics, statistical thermodynamics, and quantum thermodynamics.[11,12] The study of thermodynamics seeks to understand how energy flows within a system and how different forms of energy can be interconnected. Engineers and scientists rely on thermodynamics to design efficient energy systems, optimize processes, and develop new technologies across various fields, including chemistry, engineering, and environmental science. The thermophysical properties encompass various physical characteristics of a substance, including thermal conductivity, density, viscosity, and specific heat capacity. These properties play a crucial role in determining the solvent's efficacy across various applications, such as chemical processes, separation technologies, and energy storage systems.[13-16]

ChCl, valued for its low cost, biodegradability, and non-toxic precursor for DES, is one of the most widely used hydrogen bond acceptors in DESs. Understanding and characterizing the thermophysical properties of ChCl-based DESs is therefore a central research priority, as these properties directly influence their applicability in catalysis, extraction, and formulation processes. ChCl, a component of the B-complex vitamins, may generate eutectic mixtures with different hydrogen bond donors. These combinations provide solvents with customized characteristics that can be adjusted to fit application needs. Therefore, this investigation is vital for

*To whom correspondence should be addressed
Email: bahadur.indra@nwu.ac.za

ISSN 1996-840X Online / South African Chemical Institute / http://saci.co.za/journal
© The Author(s) Published under a Creative Commons Attribution 4.0 International Licence (CC BY 4.0)
https://doi.org/10.17159/0379-4350/2026/v80se1a03

comprehending their basic traits and enhancing their effectiveness in real-world applications.[19-22]

According to the literature, [formic acid][choline chloride] ([FA][ChCl])$_{1:2}$ is a DES that has been utilized to create functional nanocellulose through a sustainable and integrated process involving formic acid/choline chloride solvent pretreatment.[23] [FA][ChCl] is a solvent capable of solubilizing lignin, cellulose, and hemicellulose, while exhibiting high thermal stability and density.[24]

Mishra et al. examined how mono- and dicarboxylic acids influence the solvation of copper in DESs based on choline.[25] Several studies have delved into the thermodynamic properties of mixtures containing choline-based DES. For instance, Sethi et al.[26], Kiddush et al.[27] and Shekaari et al.[28] studied the excess/deviation properties of choline chloride-based DESs in water and their findings revealed negative values for both properties, indicating the predominance of intermolecular over intramolecular interactions.[26-28] Recently, Wangh et al. examined the thermodynamic characteristics of DESs including choline chloride, water, and methanol. Their study provided valuable insights into how temperature, the type of co-solvent, the choice of DES, and their concentration influence the non-ideal behavior of these pseudo-binary systems. Importantly, they observed exothermic mixing for the two DESs and methanol mixtures, though no heat was released for the mixing with water.[29]

Another study by Zuo et al. focused on choline chloride-based DESs mixed with dimethyl sulfoxide and isopropanol.[30] The researchers examined the volumetric properties, specifically the excess partial molar volume, and molar volume, as well as the excess viscosities, including logarithmic excess viscosity and viscosity deviation. Their findings demonstrated that the combination of packing effects and H-bond interactions between the DES and co-solvents led to a reduction in the volume of the mixture. Furthermore, they found that H-bond interactions played a significant role in the variations of excess viscosities. Regarding the enthalpy of mixing, they observed that the mixing of DES with isopropanol was endothermic, whereas, with dimethyl sulfoxide, it was exothermic.

Moreover, Haghbakhsh et al.[31] investigated viscosity behavior in choline chloride-based DESs mixed with alcohols such as methanol and ethanol.[31] Both systems displayed negative viscosity deviations at all examined temperatures. The negative values approached zero as temperature was raised, indicating a tendency towards more ideal behavior. It is important to note that no studies have reported measurement of thermophysical parameters for the (ChCl][FA] + methanol, or ethanol, or water) systems at various temperatures and atmospheric pressure in literature till now.

The findings of the present study have potential to provide significant information for improving efficiency and promoting environmental sustainability in many businesses as they strive to find sustainable alternatives. This research intends to facilitate valuable decision-making in the selection and design of solvents for a more environmentally friendly and sustainable future by thoroughly analyzing these features. The research comprehensively investigated the effects of temperature, DES content, and several solvents on these characteristics. Furthermore, the thermodynamic parameters that were calculated, such as the deviations in isentropic compressibilities and excess molar volumes, were precisely adjusted to conform to the Redlich-Kister equation.[32] The liquid density of the mixtures was calculated using a perturbed chain statistical associating fluid theory equation of state, specifically the PC-SAFT EoS. PC-SAFT EoS is renowned for its exceptional capability to precisely depict the behavior of associating fluids, which are frequently encountered in mixtures where molecules can establish temporary bonds or associations with one another. It makes itself a reliable choice for predicting liquid densities, particularly in systems where intermolecular interactions play a significant role.[33-35] Perturbed Chain Statistical Associating Fluid Theory (PC-SAFT)[36,37] was used for modeling the experimental data of density for the mixtures, while the Schaaff's collision theory (SCFT)[38] and Nomoto's relation (NR)[39], were employed to modeling (as predictive approach) the speed of sound in mixtures. These coupling approaches likely enhance the accuracy of the speed of sound predictions by incorporating additional factors that influence sound propagation in the fluid mixture. By involving these models (SCFT and NR) with the PC-SAFT EoS, the authors aimed to capture the intricate interplay between molecular interactions, collision dynamics, and thermodynamic properties that collectively influence the u in the mixtures under present investigation.

The selection of these models reflects a comprehensive approach for modeling the thermophysical parameters of the mixtures, considering both the complex molecular behavior and the specific phenomena relevant to sound propagation.

EXPERIMENTAL SECTION

Materials and chemicals

This research has utilized high-quality chemicals only obtained from Sigma-Aldrich (Table 1). To ensure consistent results, the samples were prepared immediately before measurements to prevent any changes caused by solvent evaporation.

Apparatus and procedure

The hydrogen-bond acceptor, ChCl, underwent a thorough drying process in an oven for 72 hours at 343.15 K, followed by placement in a desiccator.[40] The goal of drying ChCl in an oven and subsequently placing it in a desiccator is to eliminate any water molecules that might be present in or around the ChCl crystals. Removing water helps to ensure the purity and integrity of ChCl as a hydrogen-bond acceptor, allowing for more controlled and predictable interactions in experiments or applications where ChCl is being used. The absence of water prevents unintended hydrogen bonding with water molecules and helps maintain the desired properties of ChCl as a hydrogen-bond acceptor. Subsequently, the previously dried ChCl was combined with formic acid in an enclosed glass vial at a mole ratio of 1:6. This mixture was subjected to a hot plate set at T = (313 to 353) K for 6 hours until it achieved a colorless, homogeneous state. The resultant mixture was then allowed to cool to room temperature. The formulated solvent is recognised as DES and was further characterized with respect to their melting temperatures. Differential Scanning Calorimetry (SDT Q600V20.9 Build 2D) was employed for this characterization, revealing that the DES based on choline chloride and formic acid exhibited melting temperatures of 277 K. Notably, this melting temperature was lower than that of the individual components involved in the preparation of DES. It is also confirmed by literature[41] that the mixture of ChCl and FA at a mole ratio of 1:6 form DES. The formation and structure of the ChCl:FA DES were confirmed via ^{1}H NMR spectra in the literatures reported by Zhang et al.[42] and Chen et al.[43] This specific molar ratio was chosen because of their use in various chemistry and

Table 1. The criteria for pure components include the molecular weight, source, purity, and CAS number.

Chemical name	Molecular mass (g/mol)	Supplier	CAS number	Mass fraction purity
Choline chloride	139.63	Sigma-Aldrich	67-48-1	≥0.98
Formic acid	46.03	Sigma-Aldrich	64-18-6	≥0.98
Water	18.02	Produced	-	Ultrapure
Methanol	32.04	Sigma-Aldrich	67-56-1	≥0.99
Ethanol	46.07	Sigma-Aldrich	64-17-5	≥0.99

chemical engineering applications, such as direct transformation of xylose into furfural, pretreatment of biomass, the production of high-density aviation oil precursors, and in certain catalytic systems.[44,45,46] To assess the quality of the prepared mixtures (DES), their moisture content was determined using a Karl Fisher coulometer (756 KF coulometer, Metrohm, South Africa). The results indicated that the moisture content did not exceed 0.06%, underscoring the efficacy of the drying process and the meticulous preparation of the DES.

The confirmation of DES preparation was conducted by recording FTIR utilizing a Bruker Platinum ATR spectrometer equipped with the Opus 5 computer application. The instrument lens was cleaned with acetone before each operation. The FTIR spectra were shown throughout the wavelength range of 400–4000 cm^{-1}, with a remarkable resolution of 4 comprehensive accumulations and a total of 32 scans.[9] Choline chloride, formic acid, and $[ChCl][FA]_{1:6}$ DES are three different substances that have different FTIR spectra (refer to Fig.1).

Choline chloride is a salt that consists of choline cations and chloride anions. The FTIR spectrum of choline chloride shows peaks at around 3300 cm^{-1} and 1500 cm^{-1}, corresponding to the stretching and bending vibrations of the O-H and N-H bonds in the choline cations. It also shows a peak at around 1100 cm^{-1}, corresponding to the stretching vibration of the C-N bond in the choline cations. The stretching vibration of the Cl^- anions correspond with the peak at around 700 cm^{-1}.[47-49] Additionally, the peaks in the approximate range of 930–970 cm^{-1} suggest the presence of the quaternary ammonium ion within ChCl.

In the FTIR spectrum of formic acid, the peak around 1700 cm^{-1} is associated with the carbonyl stretching vibration of the C=O bond. The peak around 3300 cm^{-1} corresponds to the O-H stretching vibration of the carboxylic acid functional group, specifically the hydroxyl group (OH) in the case of formic acid. Additionally, the peak around 2900 cm^{-1} is attributed to the C-H stretching in the methyl group, and the peak around 1200 cm^{-1} corresponds to the stretching vibration of the C-O bond in the carboxylic acid.[47] Upon the creation of a DES by mixing [ChCl + FA], the resulting FTIR spectrum showcased a blend of distinctive peaks inherent to both components. The absorption bands associated with choline chloride and formic acid, previously outlined, were concurrently identified. Alterations in the intensity or location of specific bands suggested potential interactions or complex formations between molecules of chloride and formic acid. The creation of the deep eutectic solvent led to OH broadening or shifting peaks which indicated the presence of newly formed hydrogen bonds.[23,24]

The literature extensively explains the experimental process for estimating the speed of sound and density utilizing the DSA 5000M technique.[50-53] The constituents of the binary mixture (volume of 10 ml) were weighed using 0.0001 g precision OHAUS laboratory balance. The uncertainties of the mole fraction are 0.0006. The undiluted liquids were stored in sealed vials to inhibit evaporation during the creation of the binary mixtures. Afterward, the mixtures were agitated to achieve a thorough blending of all the samples. Two piezoelectric ultrasonic transducers were used to transmit the binary mixtures to determine the speed of sound. The first transducer released sound waves into the chamber holding the sample, and then the second transducer collected and recorded these waves. The transducer system enabled the measuring procedure by operating at a frequency of about 3 MHz. The DSA-5000M is equipped with temperature control mechanisms that effectively keep samples at preset temperatures with an exceptional accuracy of 0.02 K.[54] The instrument calibration was carried out with ultrapure water. The uncertainties in ρ and u are 0.0007 $g{\cdot}cm^{-3}$ and 2.83 $m{\cdot}s^{-1}$, respectively which were calculated using error propagation method. Each measurement was repeated three times to ensure the accuracy of the data.

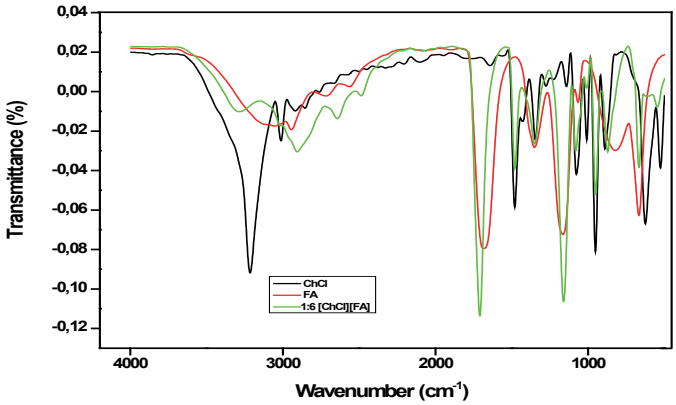


Fig. 1. FTIR spectra of [ChCl][FA], ChCl and FA.

THEORETICAL MODELS AND EQUATIONS FOR DERIVED PROPERTIES

Modeling of liquid density and speed of sound

The PC-SAFT EoS was used to simulate the density of the mixtures in this study. The existing literature documents this equation due to its demonstrated efficacy in accurately simulating a wide range of physical parameters.[33,55-61] In the references,[36,37] the reader can review in detail the equations related to PC-SAFT EoS. Five parameters are needed for this equation of state for self-associating fluid. The parameters are the following: the association energy parameter ($\varepsilon^{A_iB_i}$), the volumetric association parameter ($\kappa^{A_iB_i}$), the dispersive energy parameter (ε/k_B), the number of segments in the molecule (m), and the diameter of the segment (σ). All fluids examined in this study were analyzed using a 2B technique, which consists of both positive and negative sites. Methanol and ethanol parameters were acquired from reference,[37] while the DES and water parameters were optimized in this manuscript. For density modeling in mixtures, the binary interaction parameter (k_{ij}) must be adjusted to give the model greater flexibility and achieve better results. The binary interaction parameter corrects for attractive forces by London dispersion and can be obtained by minimizing the following objective function:

$$OF = \sum_{i=1}^{n}\left(\frac{\rho_{i,calc.} - \rho_{i,exp.}}{\rho_{i,exp.}}\right)^2 \quad (1)$$

where OF is objective function, exp. is related to the experimental value and, calc. is related to the theoretical value obtained with PC-SAFT EoS.

On the other hand, we used two models (SCFT,[38] and NR)[39] to compute the u in the binary mixtures. The u in m/s, from SCFT, can be calculated from Eq. (2):

$$u = 1600\rho\left(\sum_{i=1}^{C} x_i s_i\right)\left(\sum_{i=1}^{C} x_i N_A m_i \frac{\pi}{6} d_i^3\right) \quad (2)$$

where c denotes the number of components within the mixture, d_i signifies the molecular diameter of the component i, ρ represents the molar density for the mixture calculated using the PC-SAFT EoS, s_i (I = 1, 2) denotes the space filling factor of fluid i, x_i stands for the liquid mole fraction, and N_A is Avogadro's constant.

Also, the speed of sound may be derived from NR using Eq. (3):

$$u = \left(\frac{\sum_{i=1}^{C} \frac{x_i}{\rho_i} u_i^{\frac{1}{3}}}{\sum_{i=1}^{C} \frac{x_i}{\rho_i}}\right)^3 \quad (3)$$

where variables ρ_i and u_i correspond to the density of the pure fluid, which is determined using the PC-SAFT EoS, and the experimental u, respectively.

Equations for derived properties

This section shows the equations used to obtain derived properties such as excess and deviation characteristic, namely excess molar volume, deviation in isentropic compressibility, isentropic compressibility, and

intermolecular free length. The excess molar volumes were estimated via Eq. (4):

$$V^{E}_{m} = \frac{x_1M_1 + x_2M_2}{\rho} - \frac{x_1M_1}{\rho_1} - \frac{x_2M_2}{\rho_2} \quad (4)$$

where x_1 and x_2 are mole fractions, M_1 and M_2 are the molecular masses, ρ, $\boldsymbol{\rho}_1$ and $\boldsymbol{\rho}_2$ are the densities of solution, densities of pure components 1 and 2, respectively, '1' refers to [ChCl][FA] and '2' refers to methanol, ethanol, or water.

The calculation of isentropic compressibilities and deviations in compressibilities were performed using the following equations:

$$\kappa_s = \frac{1}{\rho u^2} \quad (5)$$

$$\Delta\kappa_s = \kappa_s - \left(x_1K_1 + x_2K_2\right) \quad (6)$$

where κ_s is isentropic compressibilities of the mixture, K_1 is the isentropic compressibility of pure component 1 ([ChCl][FA]) DES and K_2 is the pure component 2, which is water, methanol, or ethanol.

The values of intermolecular free length (L_f) for the binary mixture's values were computed using Jacobson's empirical relation:

$$L_f = K_j\left(\kappa_s\right)^{\frac{1}{2}} \quad (7)$$

where the temperature-dependent Jacobson's constant (K_j) is given as: $(93.875 + 0.375\ T)10^{-8}$.

On the other hand, the Redlich-Kister fitting parameters were calculated from Eq. (8):

$$Z = x_1x_2\sum_{i=0}^{N} A_i(2x_1 - 1)^i \quad (8)$$

where Z represents the variable V^{E}_{m} or $\boldsymbol{\Delta\kappa}_s$, x_1 represents the mole fraction of the [ChCl][FA], x_2 denotes the mole fraction of water, methanol, and ethanol, N indicates the degree of the polynomial expansion; and A_i stands for the Redlich-Kister parameters acquired for the system. The root mean square deviation was determined using Eq. (9):

$$\sigma = \left(\frac{\frac{M}{i}(Z_{exp} - Z_{cal})}{M - k}\right)^{1/2} \quad (9)$$

Z_{exp} and Z_{cal}, represent the experimental and calculated values of V^{E}_{m} or $\boldsymbol{\Delta\kappa}_s$, respectively. M is the number of experimental data points and k represents the number of coefficients employed in the Redlich-Kister correlation.

RESULTS AND DISCUSSION

In this study, we have experimentally measured the density and speed of sound of pure fluids (water, methanol, and DES) and mixtures with DES ([ChCl][FA]) at different temperatures and atmospheric pressure. Table 2 compares ρ and *u* values obtained from our present investigation with those recorded in prior literature for pure solvents. The properties of the chosen alcohol demonstrate a strong alignment with the values reported in existing literature.

The ρ of the pure DES decreases consistently as the temperature increases within the specified range. Additionally, the study explores a specific DES, [ChCl][FA], and its binary systems with water, methanol, and ethanol.

The results for these mixtures are presented in Table 3 and shown in Fig. S1, which depicts a graph of density against concentration plots for [ChCl][FA] DES at different temperatures. The observed trend is that the *ρ* of the resultant solution rises as the mole fraction of [ChCl][FA] DES in the binary systems increases. This suggests that the density of the solution is affected by the concentration of [ChCl][FA] DES in these binary systems. The non-linear nature of the shift indicates the presence of intermolecular interactions between [ChCl][FA] DES and water, methanol, and ethanol, such as Van der Waals forces or hydrogen bonds. These interactions cause a reduction in molecular distance and an increase in density. Furthermore, there is a consistent decrease in density with the increasing temperature of the binary mixture. This behavior is similar to pure DES which indicates that temperature affects the density of pure DES and binary mixtures similarly. Density is a measure of mass per unit volume, and it is affected by temperature.[62,63] In general, as the substances are heated, their molecules gain energy and move more vigorously, leading to an expansion of the substance and a decrease in density.[64,65]

The study involves measuring the speed of sound for the [ChCl][FA] DES at different concentrations. These measurements were conducted at various temperatures. The results of the experiment are presented in Fig. S2 and Table 3. The graph and table depict the correlation between the speed of sound and the concentration of [ChCl][FA] DES at different temperatures. The study compares the speed of sound for the $[ChCl][FA]_{1:6}$ DES in its pure form and in binary mixtures with water, methanol, and ethanol. It has been shown that the speed of sound decreases as the temperature increases in both the pure [ChCl][FA] DES and its binary mixture with water, methanol, and ethanol. The speed of sound tends to decrease in many liquids as temperature rises because higher temperatures often lead to increased molecular motion, which can hinder the propagation of sound waves.[66]

Excess properties were listed in Table S1 and in Fig. 2. Excess molar volumes were found to be negative in all systems ([ChCl][FA] + water, [ChCl][FA] + methanol, [ChCl][FA] + ethanol) as shown in Fig. 2.

In the context of solution thermodynamics, excess molar volume refers to the difference between the actual molar volume of a mixture and the molar volume that would be expected based on the ideal behavior of its individual components.[67] A negative excess molar volume indicates that the real molar volume of the mixture is less than what would be predicted by ideal behavior.[26-28, 68-73] This phenomenon often arises when the molecules in the mixture exhibit robust intermolecular interactions or when the molecules possess a highly organized structure that results in a decrease in the total volume of the mixture. This indicates that when [ChCl][FA] is combined with these solvents, the effective volume of the combination is less than what would be predicted based on ideal behavior. The negative excess molar volumes suggest that there are attractive interactions or structural features in these mixtures leading to a contraction in volume compared to ideal mixing behavior.

The excess molar volume values exhibit a greater magnitude of negativity as the temperature (298.15–313.15) K increases for [ChCl][FA] (x_1) + methanol and ethanol binary mixtures. Conversely, the excess molar volume values increase with an increase in temperature (298.15–313.15) K for [ChCl][FA] (x_1) + water. The decrease in excess molar volumes at higher temperatures in binary mixtures can indeed be attributed to the strengthening of intermolecular interactions among different constituents within the mixture. Higher temperatures typically enhance kinetic energy, leading to increased molecular motion and more frequent collisions between molecules. This can promote stronger intermolecular forces, resulting in denser packing and reduced excess molar volumes. Moreover, the expansion of free volume within the [ChCl][FA] molecule at higher temperatures could indeed facilitate the accommodation of a greater number of smaller methanol and ethanol molecules. This would contribute to the reduction in excess molar volumes by effectively filling up the available space between [ChCl][FA] molecules. At higher temperatures, molecules possess greater thermal energy, leading to increased molecular motion and disruption of intermolecular forces. In the context of hydrogen bonding, higher temperatures can weaken these interactions as thermal energy disrupts the organized arrangement of molecules necessary for strong hydrogen bonding to occur. Consequently, the weakening of hydrogen bonding at higher temperatures leads to an increase in excess molar volumes. This is because weaker intermolecular interactions result in a greater spatial extent of the molecules within the solution, leading to an increase in volume compared to what would be expected purely from ideal mixing

Table 2. Comparative analysis of the measured and literature values of density, ρ, and speed of sound, *u*, of pure components at T= (298.15, 303.15, 308.15, and 313.15) K. The measurements in this work were made at atmospheric pressure of 0.1 MPa.

T(K)	ρ (g·cm^{-3})		u (m·s^{-1})	
	Expt.	Lit.	Expt.	Lit.
		Water		
298.15	0.9974	0.9970 [27]	1493.95	1482.80 [27]
		0.9971 [85]		1482.84 [85]
		0.9970 [86]		1497.12 [86]
		0.9970 [50]		1497.00 [50]
		0.9971 [74]		
303.15	0.9960	0.9957 [27]	1506.25	1509.27 [27]
		0.9956 [85]		1509.25 [85]
		0.9956 [86]		1509.59 [86]
		0.9956 [87]		1509.40 [87]
		0.9956 [74]		
308.15	0.9944	0.9940 [27]	1516.89	1519.72 [27]
		0.9940 [86]		1519.82 [85]
		0.9940 [86]		1520.17 [86]
		0.9941 [74]		
313.15	0.9926	0.9922 [27]	1525.93	1528.75 [27]
		0.9922 [85]		1528.89 [90]
		0.9922 [86]		1529.25 [91]
		0.9922 [87]		
		0.9923 [74]		
		Methanol		
298.15	0.7869	0.7869 [88]	1103.17	1103.34 [88]
		0.7841 [50]		1104.30 [50]
		0.7870 [89]		1104.00 [89]
		0.7866 [90]		1102.00 [90]
		0.7883 [74]		
303.15	0.7821	0.7822 [88]	1087.16	1086.89 [88]
		0.7820 [89]		1087.10 [91]
		0.7818 [90]		1087.00 [89]
		0.7818 [87]		1086.00 [90]
		0.7835 [74]		1086.60 [87]
308.15	0.7774	0.7774 [88]	1070.73	1070.63 [88]
		0.7773 [90]		1074.00 [90]
		0.7788 [74]		
313.15	0.7726	0.7726 [88]	1054.84	1054.47 [88]
		0.7730 [89]		1054.60 [91]
		0.7728 [90]		1055.00 [89]
		0.7723 [87]		1052.00 [90]
		0.7740 [74]		1054.20 [87]
		Ethanol		
298.15	0.7862	0.7850 [89]	1143.83	1144.00 [89]
		0.7857 [90]		1149.00 [90]
		0.7853 [74]		
303.15	0.7817	0.7810 [89]	1127.06	1127.00 [89]
		0.7820 [91]		1128.00 [90]
		0.7811 [87]		1128.20 [87]
		0.7812 [74]		
308.15	0.7776	0.7777 [90]	1110.33	1098.00 [90]
313.15	0.7732	0.7720 [89]	1093.64	1094.00 [89]
		0.7736 [91]		1086.00 [91]
		0.7723 [87]		1094.60 [87]
		0.7724 [74]		
		$[ChCl][FA]_{1:6}$		
298.15	1.1521		1831.84	
303.15	1.1489		1819.90	
308.15	1.1457		1807.81	
313.13	1.1425		1795.81	

The standard uncertainties for temperature (T) and pressure (p) are 0.02 K and 0.04 MPa, respectively. The combined expanded uncertainties for mole fraction (x), density (ρ), and speed of sound (u) are Uc(x) = 0.0006, Uc(ρ) = 0.0007 g·cm^{-3}, and Uc(u) = 2.83 m·s^{-1}, respectively, at a 0.95 level of confidence.

behavior. A similar effect of temperature on excess molar volume values in choline based DESs has been reported in the literature.[26,27,74-76]

The $V^{E}_{m,min}$ occured at x_1 = 0.4000 for water, and for methanol and ethanol, it was at x_1 = 0.4000 and 0.6000 across all temperatures. This phenomenon arises when the constituents in the mixture form stable relationships with one another.

The concept of isentropic compressibility, κ_s, refers to the quantification of a substance's susceptibility to compression in the absence of heat exchange.[77] Table 3 and Fig. S3 present the isentropic compressibility values, κ_s, for the binary systems of [ChCl][FA] DES in water, methanol, and ethanol at different temperatures.

Fig. S3 illustrates the relationship between the findings and the mole fractions of [ChCl][FA] DES at all temperatures. Isentropic compressibility values have been determined to be consistently positive across the entire range of composition and experimental temperatures in all binary mixtures. The observed trend indicates that isentropic compressibilities decrease with an increase in the mole fraction (x_1) and conversely increase with the rise in temperature. This pattern of variation in κ_s is likely attributed to a closer proximity of unlike molecules within the mixtures and a strengthening of interactions between the components. Isentropic compressibility is a measure of how much a substance's volume changes under pressure while maintaining constant entropy (i.e., without producing heat). Positive values of isentropic compressibility indicate that the substance or material is easily compressible under certain conditions. Isentropic compressibility measures the relative volume change of a substance in response to a change in pressure while maintaining constant entropy. So, a positive value suggests that an increase in pressure leads to a decrease in volume, indicating compressibility. Understanding these interactions can provide insights into the behavior of the substance or mixture under different conditions.[78,79]

Based on the results presented in Fig. 3 and Table S1, the deviation in isentropic compressibility values exhibits a consistent negative deviation for mixtures of [ChCl][FA] in a ratio DES with methanol and ethanol at temperatures of (298.15 and 313.15) K. Negative deviation implies that the observed isentropic compressibility is lower than what ideal behavior would predict. In other words, the actual volume change in response to pressure is less than expected. The negative deviations in isentropic compressibility across all systems might arise from reduced intermolecular free lengths and higher speed of sound. [26-28, 68-72] This indicates that the combination is less able to be compressed compared to the ideal mixture. This suggests that there may be a significant connection between the $[ChCl][FA]_{1:6}$ DES and the water, methanol, and ethanol at the molecular level. However, a

Table 3. Density, ρ, speed of sound, u, isentropic compressibility and intermolecular free length, Lf, for the binary mixture {[ChCl][FA] (x1) + water, methanol, and ethanol (x2)} at T = (298.15, 303.15, 308.15, and 313.15) K and atmospheric pressure (0.1 MPa).

x_1	ρ/(g cm^{-3})	u /(m·s^{-1})	κ_s/ (TPa^{-1}) × 10^{-2}	L_f (nm)× 10^2
{[ChCl][FA] (x_1) + water (x_2)}				
T = 298.15				
0.0000	0.9974	1493.95	4.49	4.36
0.2237	1.0755	1597.81	3.64	3.93
0.3791	1.1040	1672.48	3.24	3.70
0.5779	1.1265	1775.86	2.81	3.45
0.7012	1.1363	1810.12	2.69	3.37
0.7851	1.1416	1813.03	2.66	3.36
0.8456	1.1451	1814.78	2.65	3.35
0.8915	1.1474	1815.77	2.64	3.34
0.9274	1.1492	1816.57	2.64	3.34
0.9564	1.1505	1817.15	2.63	3.34
0.9801	1.1515	1817.94	2.63	3.33
1.0000	1.1521	1831.84	2.59	3.31
T = 303.15				
0.0000	0.9960	1506.25	4.43	4.37
0.2237	1.0727	1594.82	3.67	3.97
0.3791	1.1009	1665.32	3.28	3.76
0.5779	1.1233	1766.33	2.85	3.51
0.7012	1.1331	1799.58	2.73	3.43
0.7851	1.1383	1802.06	2.71	3.41
0.8456	1.1418	1803.51	2.69	3.41
0.8915	1.1442	1804.34	2.68	3.40
0.9274	1.1459	1805.00	2.68	3.40
0.9564	1.1472	1805.48	2.67	3.39
0.9801	1.1483	1806.16	2.67	3.39
1.0000	1.1489	1819.90	2.63	3.36
T = 308.15				
0.0000	0.9944	1516.89	4.37	4.38
0.2237	1.0698	1591.25	3.69	4.02
0.3791	1.0978	1657.70	3.31	3.81
0.5779	1.1201	1756.17	2.89	3.56
0.7012	1.1297	1788.30	2.77	3.48
0.7851	1.1351	1790.68	2.75	3.47
0.8456	1.1385	1791.84	2.74	3.46
0.8915	1.1409	1792.55	2.73	3.46
0.9274	1.1427	1793.16	2.72	3.46
0.9564	1.1440	1793.58	2.72	3.45
0.9801	1.1450	1794.19	2.71	3.45
1.0000	1.1457	1807.81	2.67	3.42
T = 313.15				
0.0000	0.9926	1525.93	4.33	4.40
0.2237	1.0668	1587.11	3.72	4.08
0.3791	1.0946	1649.70	3.36	3.87
0.5779	1.1168	1745.66	2.94	3.62
0.7012	1.1264	1776.93	2.81	3.54
0.7851	1.1318	1779.21	2.79	3.53
0.8456	1.1353	1780.19	2.78	3.52
0.8915	1.1376	1780.79	2.77	3.52
0.9274	1.1394	1781.29	2.77	3.51
0.9564	1.1407	1781.68	2.76	3.51
0.9801	1.1418	1782.34	2.76	3.51
1.0000	1.1425	1795.81	2.71	3.48
{[ChCl][FA] (x_1) + methanol (x_2)}				
T = 298.15				
0.0000	0.7869	1103.17	10.44	6.65
0.2234	0.9019	1287.98	6.68	5.32
0.3790	0.9683	1420.25	5.12	4.65
0.5781	1.0424	1579.19	3.85	4.03
0.7005	1.0810	1679.06	3.28	3.73
0.7850	1.1049	1738.77	2.99	3.56
0.8434	1.1201	1767.08	2.86	3.48
0.8911	1.1309	1789.38	2.76	3.42
0.9271	1.1378	1796.15	2.72	3.39
0.9551	1.1419	1801.18	2.70	3.38
1.0000	1.1521	1831.84	2.59	3.31
T = 303.15				
0.0000	0.7821	1087.16	10.82	6.83
0.2234	0.8979	1274.34	6.86	5.44
0.3790	0.9645	1407.30	5.24	4.75
0.5781	1.0388	1566.83	3.92	4.11
0.7005	1.0776	1666.47	3.34	3.79
0.7850	1.1016	1726.50	3.05	3.62
0.8434	1.1169	1754.83	2.91	3.54
0.8911	1.1278	1775.39	2.81	3.48
0.9271	1.1347	1783.68	2.77	3.45
0.9551	1.1387	1789.66	2.74	3.44
1.0000	1.1489	1819.90	2.63	3.36
T = 308.15				
0.0000	0.7774	1070.73	11.22	7.02
0.2234	0.8940	1260.91	7.04	5.56
0.3790	0.9608	1394.31	5.35	4.85
0.5781	1.0354	1554.95	3.99	4.19
0.7005	1.0743	1653.85	3.40	3.86
0.7850	1.0982	1713.97	3.10	3.69
0.8434	1.1137	1742.98	2.96	3.60
0.8911	1.1246	1764.26	2.86	3.54
0.9271	1.1316	1771.30	2.82	3.51
0.9551	1.1356	1778.30	2.78	3.49
1.0000	1.1457	1807.81	2.67	3.42
T = 313.15				
0.0000	0.7726	1054.84	11.63	7.21
0.2234	0.8900	1247.70	7.22	5.68
0.3790	0.9570	1381.45	5.48	4.94
0.5781	1.0321	1543.70	4.07	4.26
0.7005	1.0708	1639.64	3.47	3.94

Table 3. Continued.

x_1	ρ/(g cm^{-3})	u /(m·s^{-1})	κ_s/ (TPa^{-1}) × 10^{-2}	L_f (nm)× 10^2
{[ChCl][FA] (x_1) + water (x_2)}				
T = 313.15				
0.7850	1.0949	1701.39	3.16	3.75
0.8434	1.1104	1731.59	3.00	3.66
0.8911	1.1215	1752.28	2.90	3.60
0.9271	1.1284	1758.81	2.86	3.58
0.9551	1.1325	1767.88	2.83	3.55
1.0000	1.1425	1795.81	2.71	3.48
{[ChCl][FA] (x_1) + ethanol (x_2)}				
T = 298.15				
0.0000	0.7862	1143.83	9.72	6.41
0.2243	0.8701	1260.68	7.23	5.53
0.3781	0.9276	1349.11	5.92	5.01
0.5779	1.0010	1478.99	4.57	4.40
0.7016	1.0459	1584.20	3.81	4.01
0.7846	1.0761	1665.64	3.35	3.76
0.8456	1.0983	1720.84	3.07	3.61
0.8913	1.1141	1758.58	2.90	3.50
0.9274	1.1265	1779.89	2.80	3.44
0.9554	1.1361	1765.12	2.83	3.46
0.9800	1.1446	1811.09	2.66	3.36
0.9904	1.1484	1818.41	2.63	3.34
1.0000	1.1521	1831.84	2.59	3.31
T = 303.15				
0.0000	0.7817	1127.06	10.07	6.59
0.2243	0.8660	1245.04	7.45	5.66
0.3781	0.9237	1333.97	6.08	5.12
0.5779	0.9973	1464.25	4.68	4.49
0.7016	1.0424	1569.97	3.89	4.09
0.7846	1.0726	1653.19	3.41	3.83
0.8456	1.0949	1706.28	3.14	3.68
0.8913	1.1107	1745.64	2.95	3.57
0.9274	1.1232	1767.89	2.85	3.50
0.9554	1.1328	1781.66	2.78	3.46
0.9800	1.1413	1798.86	2.71	3.42
0.9904	1.1452	1798.90	2.70	3.41
1.0000	1.1489	1819.90	2.63	3.36
T = 308.15				
0.0000	0.7776	1110.33	10.43	6.76
0.2243	0.8619	1229.18	7.68	5.80
0.3781	0.9198	1318.55	6.25	5.24
0.5779	0.9936	1449.21	4.79	4.58
0.7016	1.0388	1555.67	3.98	4.18
0.7846	1.0693	1640.84	3.47	3.90
0.8456	1.0915	1692.80	3.20	3.74
0.8913	1.1074	1732.70	3.01	3.63
0.9274	1.1200	1755.92	2.90	3.56
0.9554	1.1295	1769.27	2.83	3.52
0.9800	1.1381	1786.70	2.75	3.47
0.9904	1.1420	1786.92	2.74	3.47
1.0000	1.1457	1807.81	2.67	3.42
T = 313.15				
0.0000	0.7732	1093.64	10.81	6.95
0.2243	0.8578	1213.35	7.92	5.95
0.3781	0.9158	1303.09	6.43	5.36
0.5779	0.9899	1434.17	4.91	4.68
0.7016	1.0354	1541.55	4.06	4.26
0.7846	1.0660	1628.78	3.54	3.97
0.8456	1.0878	1679.49	3.26	3.81
0.8913	1.1041	1719.83	3.06	3.70
0.9274	1.1168	1744.25	2.94	3.63
0.9554	1.1263	1756.98	2.88	3.58
0.9800	1.1349	1774.64	2.80	3.53
0.9904	1.1388	1775.08	2.79	3.53
1.0000	1.1425	1795.81	2.71	3.48

The standard uncertainties for temperature (T) and pressure (p) are 0.02 K and 0.04 MPa, respectively. The combined expanded uncertainties for mole fraction (x), density (ρ), and speed of sound (u) are Uc(x) = 0.0006, Uc(ρ) = 0.0007 g·cm^{-3}, and Uc(u) = 2.83 m·s^{-1}, respectively, at a 0.95 level of confidence.

notable shift occurs as these deviations shows transition from negative to positive when [ChCl][FA] DES is mixed with water and ethanol at temperatures of (303.15 and 308.15) K. A positive deviation suggests that the observed isentropic compressibility is higher than what would be predicted by ideal behavior.[80] In this case, the actual volume change in response to pressure is greater than expected. Positive deviations suggest repulsive forces, leading to a larger volume change than predicted. The shift from negative to positive deviations may indicate changes in the dominant intermolecular interactions.

As temperature rises, the deviation in isentropic compressibility values for binary mixtures of methanol and ethanol (298.15 K and 313.15 K) become increasingly negative. It suggests that the interactions between the molecules in the mixture are becoming stronger, leading to more non-ideal behavior.[81, 82] As temperature increases, molecular motion becomes more vigorous. Stronger intermolecular forces, such as hydrogen bonding or other specific interactions, may become more pronounced at higher temperatures. This can lead to a more negative deviation in isentropic compressibility. Changes in temperature can influence the molecular structure of the components in the mixture. For instance, conformational changes or alterations in molecular packing can affect the compressibility of the mixture. Temperature change can affect the effective size and shape of molecules. This can impact on how molecules pack together and interact, influencing the compressibility of the mixture. Changes in temperature can also affect the density of the mixture. Change in density can influence compressibility, especially if the mixture undergoes phase transitions or significant changes in molecular arrangement. As the temperature increases for binary mixtures of water and ethanol (at 308.15 K and 303.15 K), the deviation in isentropic compressibility values shifts from being more positive to more negative. The reasons for this behavior could be related to the molecular interactions and thermodynamic properties of the components in the mixture.

The $\Delta\kappa_{s,min}$ occurred at x_1 = 0.6000 for water and at x_1 = 0.4000 for methanol and ethanol at all temperatures. The minimum deviation at x_1 = 0.4000 indicates more consistent behavior. The minimum

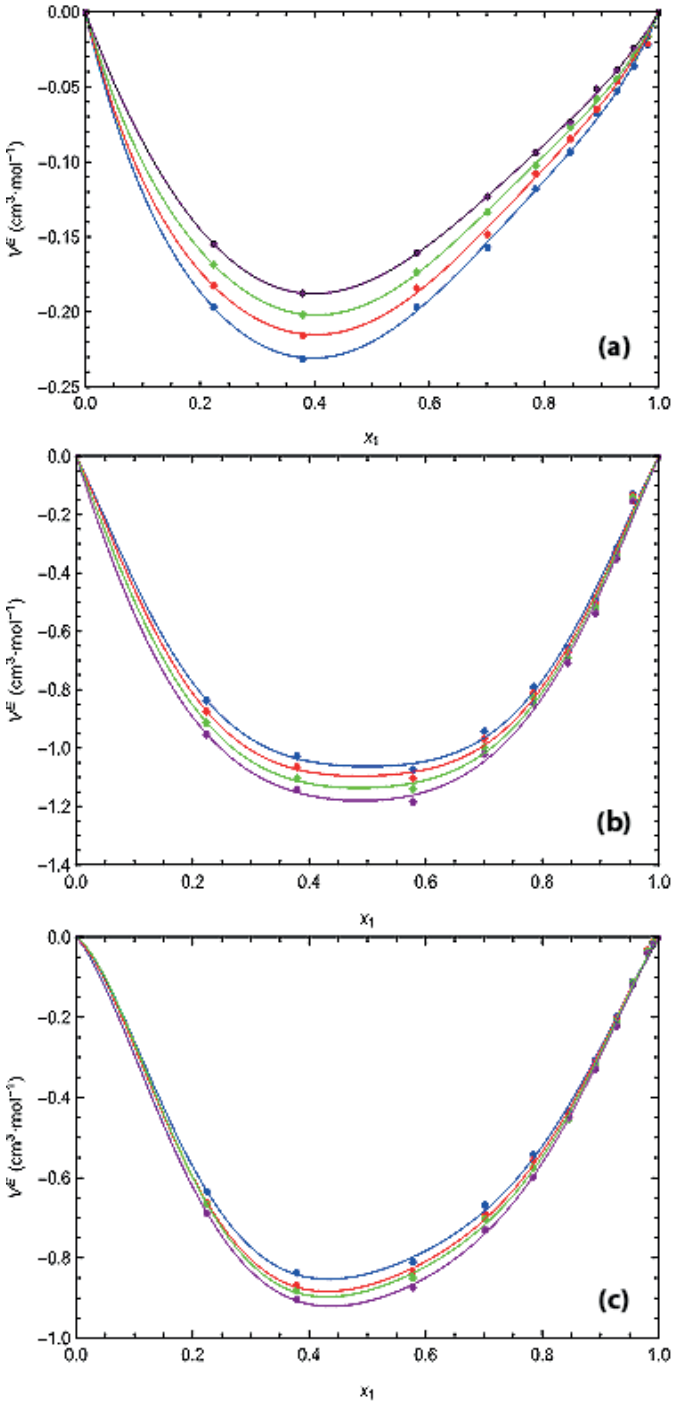


Fig. 2. Experimental excess molar volumes, V_m^E, and calculated using Redlich-Kister model for the binary mixtures of {[ChCl[FA] (x_1) + water (a), methanol (b), and ethanol (c)} at 298.15 K (blue), 303.15 K (red), 308.15 K (green), 313.15 K (purple).Circles represent the experimental data, and the solid lines were generated using the Redlich-Kister smoothing polynomial.

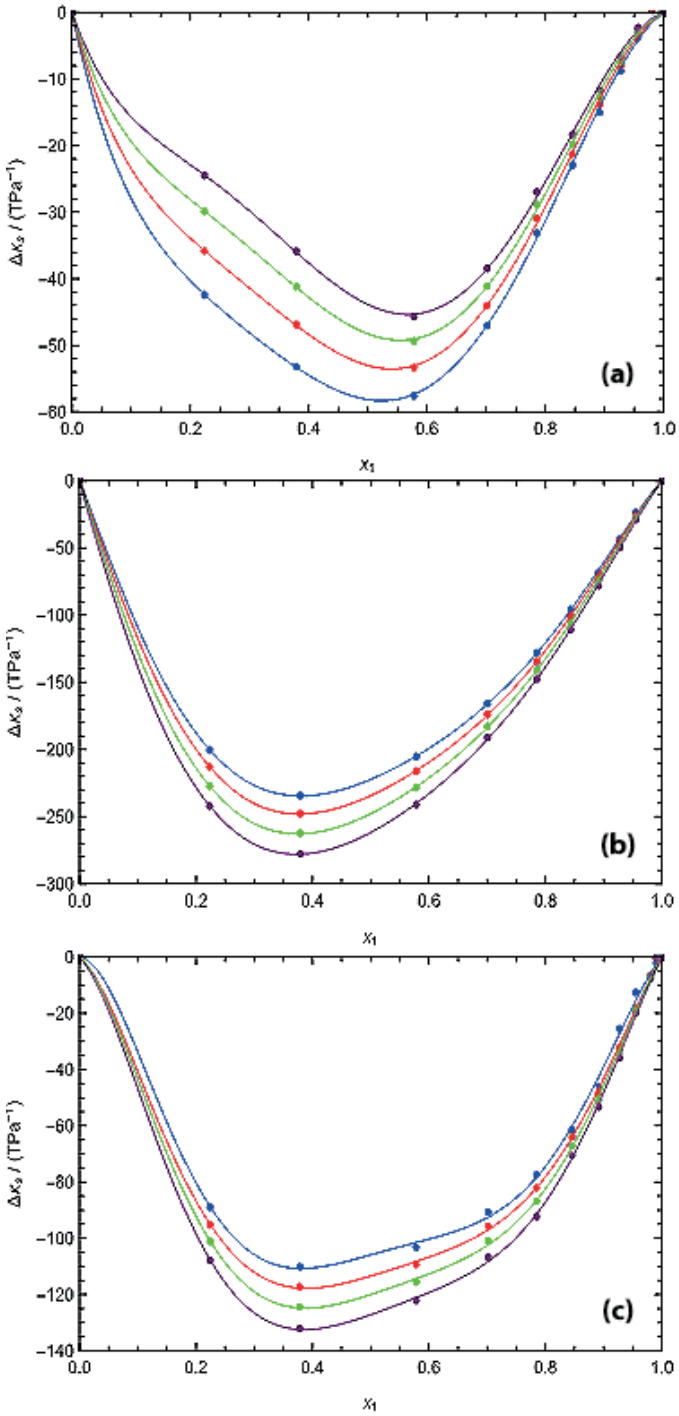


Fig. 3. Experimental excess isentropic compressibilities, Δ and calculated using Redlich-Kister for the binary mixtures of {[ChCl[FA] (x_1)+ water (a), methanol (b), and ethanol (c)} at 298.15 K (blue), 303.15 K (red), 308.15 K (green), 313.15 K (purple).Circles represent the experimental data, and the solid lines were generated using the Redlich-Kister smoothing polynomial.

deviations at specific mole fractions indicate the points where the interactions between the molecules in the mixture are minimized, resulting in behavior closer to ideal mixing.

The mole fraction of [ChCl][FA] in the ratio rises with a decrease in the intermolecular free length values (calculated using the equation given in literature[83,84]), as elucidated in Table 3 and Fig. S4. This phenomenon may be explained in terms of the addition of more solvent molecules to the mixture, which results in an increase in the interactions between molecules, consequently resulting in a closer arrangement and a decrease in the average distance between molecules. The correlation between the values of intermolecular free length and temperature is also significant. As the temperature rises, the values of intermolecular free length show an increasing tendency. This tendency may be attributed to the fact that the increased thermal energy of the molecules at higher temperature, results in their accelerated movement and expanded spatial occupation. Consequently, the average distance between molecules expands due to the increased kinetic energy and molecular motion associated with higher temperatures.

The Redlich-Kister fitting smoothing polynomial was used to determine the fitting parameters of the binary systems, together with their corresponding standard deviations (Table 4).[32] The Redlich-

Kister smoothing equation effectively correlated the variables V_m^E and $\Delta\kappa_s$, providing a comprehensive understanding of correlation process.

Further, the results related to the application of PC-SAFT EoS, and the speed of sound models have been discussed. The parameters for DES and water were optimized in this article, using the objective function recommended by Gross and Sadowski.[36] In the case of DES, as we assume it to be a pseudo pure fluid, there is no experimental vapor pressure data available. As a result, we used our collected liquid density data and the DIPPR-published vapor pressure data (for only water) to optimize the parameters. The optimal parameters are depicted in Table 5.

According to this table, both the vapor pressure and the liquid density are well adjusted for both the fluids. In order to model the liquid density for the binary mixtures and subsequently calculating the speed of sound, it was necessary to adjust the binary interaction parameter. The optimal binary parameters are published in Table 6, along with the respective deviations.

According to Table 6, the binary parameters are negative, and only one fitted parameter was needed for each mixture to correctly represent the density of the liquid mixtures (overall deviation = 0.16%). On the other hand, both models (SCFT and NR) are capable of quantitatively representing the *u* of the mixtures. Among these

Table 4. Redlich-Kister fitting parameters and root-mean-square deviation, *σ*, for the binary mixtures at various temperatures and atmospheric pressure (0.1 MPa).

	A_i	293.15 K	303.15 K	308.15 K	313.15 K
{[ChCl][FA] (x_1) + water (x_2)}					
V_m^E/(cm³·mol⁻¹)	A_0	-0.879	-0.825	-0.772	-0.714
	A_1	0.406	0.362	0.360	0.349
	A_2	-0.019	0.013	0.057	0.001
	A_3	-0.056	-0.011	-0.083	-0.154
	A_4	-0.375	-0.364	-0.330	-0.119
	σ	0.003	0.003	0.002	0.002
$\Delta\kappa_s$/(TPa⁻¹)	A_0	-232.559	-212.016	-193.009	-175.373
	A_1	-27.731	-49.082	-67.423	-84.218
	A_2	44.035	60.671	74.718	85.371
	A_3	208.324	204.996	200.609	197.020
	A_4	-52.661	-53.220	-52.248	-48.584
	σ	0.870	0.887	0.902	0.908
{[ChCl][FA] (x_1) + methanol(x_2)}					
V_m^E/(cm³·mol⁻¹)	A_0	-4.253	-4.382	-4.545	-4.721
	A_1	-0.001	0.082	0.107	0.108
	A_2	-2.682	-2.831	-2.684	-2.426
	A_3	0.115	0.093	0.339	0.664
	A_4	3.037	3.038	2.465	1.688
	σ	0.031	0.033	0.033	0.034
$\Delta\kappa_s$/(TPa⁻¹)	A_0	-889.213	-937.563	-991.318	-1047.170
	A_1	367.181	396.399	427.575	460.029
	A_2	-361.121	-382.281	-398.740	-402.951
	A_3	-48.296	-34.461	-7.883	22.593
	A_4	428.595	430.904	403.566	352.249
	σ	0.938	0.780	0.858	1.014
{[ChCl][FA] (x_1) + ethanol(x_2)}					
V_m^E/(cm³·mol⁻¹)	A_0	-3.358	-3.475	-3.528	-3.634
	A_1	0.747	0.798	0.817	0.732
	A_2	-1.137	-1.200	-1.264	-1.161
	A_3	-1.340	-1.330	-1.543	-1.160
	A_4	2.698	2.817	3.086	2.681
	σ	0.012	0.012	0.012	0.009
$\Delta\kappa_s$/(TPa⁻¹)	A_0	-423.514	-453.649	-479.911	-508.504
	A_1	115.821	123.844	135.133	145.841
	A_2	-419.116	-365.372	-389.149	-415.478
	A_3	-235.753	-218.546	-232.852	-240.266
	A_4	701.838	539.722	574.154	605.302
	σ	1.969	1.598	1.635	1.693

The standard uncertainties for temperature (T) and pressure (p) are 0.02 K and 0.04 MPa, respectively. The combined expanded uncertainties for mole fraction (*x*), density (ρ), and speed of sound (*u*) are Uc(*x*) = 0.0006, Uc(ρ) = 0.0007 g·cm⁻³, and Uc(*u*) = 2.83 m·s⁻¹, respectively, at a 0.95 level of confidence.

Table 5. Parameters of the pure fluids (required in PC-SAFT EoS) that were optimized in this manuscript and the absolute average deviation in liquid density and vapor pressure.

Fluid	m	σ / (Å)	ε/k_B / (K)	ε^{AB}/k_B / (K)	κ^{AB}	%AADρ	%AADP
[ChCl][FA]	2.7703	2.9971	306.3907	6825.68	0.1312	0.08	-
Water	1.0774	2.9102	367.5276	2598.92	0.0268	0.15	0.03

$\%AAD\varphi = \frac{100}{N}\sum_{i=1}^{n}\frac{\left|\varphi_{i,exp.} - \varphi_{i,calc.}\right|}{\varphi_{i,exp.}}, \varphi = \rho \text{ or } P, n$ is the number of the experimental points, exp. is related to the experimental value, and calc. is related to the theoretical value obtained with PC-SAFT EoS. In the case of vapor pressure, exp. must be replaced by DIPPR.

Table 6. Fitted binary parameters and the absolute average deviation for liquid density and speed of sound considering two theoretical models.

Mixture	k_{ij}	%AADρ	%AAD*u* using SCFT	%AADu using NR
{[ChCl][FA] (x_1) + water (x_2)}	-0.1320	0.07	1.71	0.97
{[ChCl][FA] (x_1) + methanol (x_2)}	-0.0249	0.36	1.59	2.04
{[ChCl][FA] (x_1) + ethanol (x_2)}	-0.0174	0.06	1.76	0.68
Overall		0.16	1.69	1.23

$\%AAD\varphi = \frac{100}{N}\sum_{i=1}^{n}\frac{\left|\varphi_{i,exp.} - \varphi_{i,calc.}\right|}{\varphi_{i,exp.}}, \varphi = \rho \text{ or } u, n$ is the number of the experimental points, exp. is related to the experimental value, and calc. is related to the theoretical value.

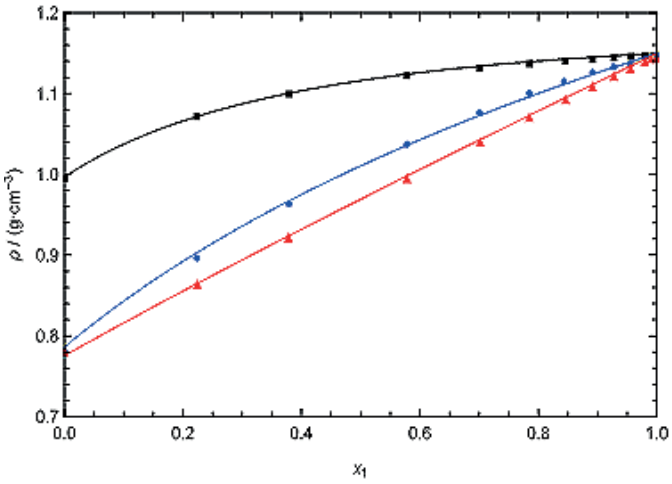


Fig. 4. Comparison between experimental density and calculated density using PC-SAFT EoS at 303.15 K. Symbols: (black ■){[ChCl][FA] (x_1) + water (x_2)} , (blue ●){[ChCl][FA]$_{1:6}$ (x_1) + methanol (x_2)}, (red ▲){[ChCl][FA] (x_1) + ethanol (x_2)}. Solid lines represent results obtained from PC-SAFT EoS.

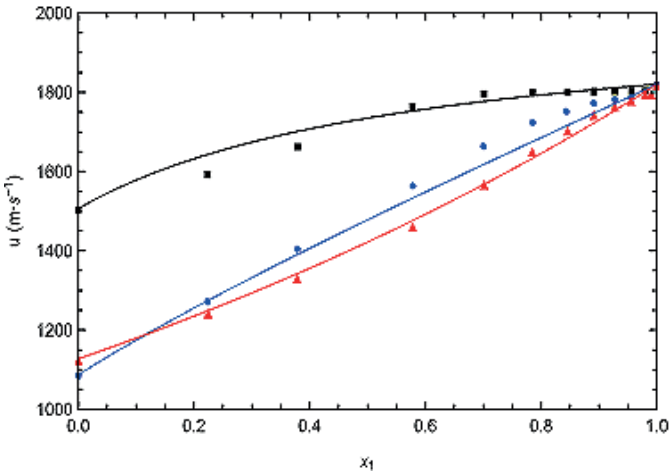


Fig. 5. Comparison between experimental speed of sound and calculated speed of sound using PC-SAFT EoS at 303.15 K. Symbols: (black ■) {[ChCl][FA] (x_1) + water (x_2)} , (blue ●) {[ChCl][FA] (x_1) + methanol (x_2)}, (red ▲) {[ChCl][FA] (x_1) + ethanol (x_2)}. Black and red lines represent results obtained from PC-SAFT EoS + NR and blue line represent results obtained from PC-SAFT EoS + SCFT.

models, the best was NR, with an overall deviation of 1.23%. The best results were obtained with NR for the mixtures {[ChCl][FA] (x_1) + ethanol (x_2)} (0.68%) and {[ChCl][FA]$_{1:6}$ (x_1) + water (x_2)} (0.97%). Fig. 4 shows the comparison between experimental ρ and ρ calculated from PC-SAFT EoS at 303.15 K; PC-SAFT EoS correctly models the ρ for all three binary mixtures.

On the other hand, Fig. 5 shows the variation in *u* for all mixtures at 303.15 K. According to these results, the *u* increases with the x_1 for all the mixtures at 303.15 K. Furthermore, the best model for each combination accurately captured the relationship between the *u* and the x_1.

CONCLUSION

This study investigated the thermophysical properties of choline-based deep eutectic solvents, specifically the binary system [ChCl][FA] with methanol, ethanol, and water in the temperature range 293.15–323.15 K at atmospheric pressure. Density (ρ) and ultrasonic velocity (u) showed clear temperature-dependent trends, reflecting the role of molecular interactions. Negative excess molar volumes indicated predominant attractive interactions, while deviations in isentropic compressibility revealed a shift from attractive to repulsive forces with increasing temperature. The Redlich-Kister correlation was effectively used for correlating excess molar volumes and deviation in isentropic compressibility. PC-SAFT EoS accurately predicted the density of the binary mixtures with an overall deviation of 0.16%. On the other hand, the speed of sound models allowed the speed of sound to be correctly modeled; the overall deviation with SCFT and NR were 1.69% and 1.23%, respectively. These results provide reliable thermophysical data that can support the design and application of deep eutectic solvents in industrial processes.

SUPPLEMENTARY MATERIAL

Supplementary tables and figures associated with this article are available in a separate pdf.

FUNDING ACKNOWLEDGEMENT

I. Bahadur thanks the SASOL South Africa for funding. The KSU author acknowledge the funding from Ongoing Research Funding Program-Research Chairs (ORF-RC-2026-0200), King Saud University, Riyadh, Saudi Arabia. A.H. acknowledges the economic support given by the UDLA.

AUTHOR CONTRIBUTIONS

Sibusiso Msimanga: Experimental measurements and analysis of the results; **Ncomeka Mgxadeni:** Experimental measurements, analysis of the results, and participating to the paper preparation; **Ariel Hernández:** modeling with PC-SAFT and Redlich-Kister. **Indra Bahadur:** Supervision, Mentoring, Management of the research team, Writing – review & editing, Addressing the comments from reviewers, Conceptualization, Visualization, Validation; **Shailendra Kumar Singh:** Participating to the paper preparation; **Faruq Mohammad:** Writing – review & editing, Visualization, Resources, Funding acquisition. **Sangeeta Singh:** DES preparation, characterization and participating to the paper preparation **Kaniki Tumba:** Evaluation of the experimental data, mentoring, and participating to the paper preparation; **Ahmed Abdullah Soleiman**: Writing – review & editing, Visualization, Validation.

STATEMENT OF COMPETING INTEREST

The authors declare no competing interest.

DECLARATION OF GENERATIVE AI AND AI-ASSISTED TECHNOLOGIES

During the preparation of this work, the author(s) used Grammarly to check and proofread grammatical mistakes and punctuation. After using this tool/service, the author(s) reviewed and edited the content as needed and took(s) full responsibility for the content of the publication.

ORCID IDS

Sibusiso Msimanga: https://orcid.org/0000-0001-7188-960X
Ncomeka Mgxadeni: https://orcid.org/0000-0001-6188-3925
Ariel Hernández: https://orcid.org/0000-0002-6120-9444
Indra Bahadur: https://orcid.org/0000-0003-2906-473X
Faruq Mohammad: https://orcid.org/0000-0002-9318-9986
Ahmed Abdullah Soleiman: https://orcid.org/0009-0003-2361-8153

REFERENCES

1. Abbott AP. Deep eutectic solvents and their application in electrochemistry. Curr Opin Green Sustain Chem. 2022;36:100649. https://doi.org/10.1016/j.cogsc.2022.100649.
2. Meenu M, Bansal V, Rana S, Sharma N, Kumar V, Arora V, Garg M. Deep eutectic solvents (DESs) and natural deep eutectic solvents (NADESs): designer solvents for green extraction of anthocyanin. Sustain Chem Pharm. 2023;34:101168. https://doi.org/10.1016/j.scp.2023.101168.
3. Cichowska-Kopczyńska I, Nowosielski B, Warmińska D. Deep eutectic solvents: properties and applications in CO2 separation. Molecules. 2023;28(14):5293. https://doi.org/10.3390/molecules28145293.
4. Wu H, Zhang X, Xiong W, Liang J, Zhang S, Hu X, Wu Y. Deep eutectic behavior in binary mixtures of protic ionic liquids. J Mol Liq. 2022;366:120251. https://doi.org/10.1016/j.molliq.2022.120251.
5. Abbott AP, Capper G, Davies DL, Rasheed RK, Tambyrajah V. Novel solvent properties of choline chloride/urea mixturesElectronic supplementary information (ESI) available: spectroscopic data. See http://www.rsc.org/suppdata/cc/b2/b210714g/". Chem Commun (Camb). 2003;70(1):70–71. https://doi.org/10.1039/b210714g.
6. Abbott AP, Capper G, Davies DL, Munro HL, Rasheed RK, Tambyrajah V. Preparation of novel, moisture-stable, Lewis-acidic ionic liquids containing quaternary ammonium salts with functional side chains. Chem Commun (Camb). 2001;19(19):2010–2011. https://doi.org/10.1039/b106357j.
7. Abbott AP, Capper G, Davies DL, Rasheed RK. Ionic liquid analogues formed from hydrated metal salts. Chemistry. 2004;10(15):3769–3774. https://doi.org/10.1002/chem.200400127.
8. Mgxadeni N, Kabane B, Bahadur I, Varma RS, Singh S. Deep eutectic solvents as sustainable solvents for industrial separation problems. A recent update. J Ion Liq. 2023;3(2):100065. https://doi.org/10.1016/j.jil.2023.100065.
9. Mgxadeni N, Kabane B, Bahadur I, Paredes ML, Soares RdeP. Singh, SK, Mohammad F, Soleiman AA. Thermodynamic properties, activity coefficients at infinite dilution and cosmo-SAC modelling of deep eutectic solvents at different temperatures. ChemistrySelect. 2023;8:e202204192. https://doi.org/10.1002/slct.202204192.
10. Mgxadeni N, Mmelesi O, Kabane B, Bahadur I. Influence of hydrogen bond donor on zinc chloride in separation of binary mixtures: activity coefficients at infinite dilution. J Mol Liq. 2022;351:118596. https://doi.org/10.1016/j.molliq.2022.118596.
11. Gyftopoulos EP, Beretta GP. Thermodynamics: foundations and applications. Courier Corporation; 2022. https://doi.org/10.1016/j.molliq.2022.118596.
12. Haddad WM. Thermodynamics: the unique universal science. Entropy (Basel). 2017;19(11):621. https://doi.org/10.3390/e19110621.
13. Fabre E, Murshed SS. A review of the thermophysical properties and potential of ionic liquids for thermal applications. J Mater Chem A Mater Energy Sustain. 2021;9(29):15861–15879. https://doi.org/10.1039/D1TA03656D.
14. Zhang FF, Zheng FF, Wu XH, Yin YL, Chen G. ariations of thermophysical properties and heat transfer performance of nanoparticle-enhanced ionic liquids. R Soc Open Sci. 2019;6(4):182040. https://doi.org/10.1098/rsos.182040.
15. Dehury P, Singh J, Banerjee T. Thermophysical and Forced convection studies on (alumina + menthol)-based deep eutectic solvents for their use as a heat transfer fluid. ACS Omega. 2018;3(12):18016–18027. https://doi.org/10.1021/acsomega.8b02661.
16. Dey D, Kumar P, Samantaray S. A review of nanofluid preparation, stability, and thermo-physical properties. Heat Transf Asian Res. 2017;46(8):1413–1442. https://doi.org/10.1002/htj.21282.
17. Şahin S, Pharm J. Tailor-designed deep eutectic liquids as a sustainable extraction media: an alternative to ionic liquids. J Pharm Biomed Anal. 2019;174:324–329. https://doi.org/10.1016/j.jpba.2019.05.059.
18. Haghbakhsh R, Raeissi S. Densities and volumetric properties of (choline chloride+ urea) deep eutectic solvent and methanol mixtures in the temperature range of 293.15–323.15 K. J Chem Thermodyn. 2018;124:10–20. https://doi.org/10.1016/j.jct.2018.04.010.
19. Cea-Klapp E, Garrido JM, Quinteros-Lama H. Insights into the orientation and hydrogen bond influence on thermophysical and transport properties in choline-based deep eutectic solvents and methanol. J Mol Liq. 2022;345:117019. https://doi.org/10.1016/j.molliq.2021.117019.
20. Sazali AL, AlMasoud N, Amran SK, Alomar TS, Paèe KF, El-Bahy ZM, Yong TLK, Dailin DJ, Chuah LF. Physicochemical and thermal characteristics of choline chloride-based deep eutectic solvents. Chemosphere. 2023;338:139485. https://doi.org/10.1016/j.chemosphere.2023.139485.
21. Alkhatib II, Bahamon D, Llovell F, Abu-Zahra MR, Vega LF. Perspectives and guidelines on thermodynamic modelling of deep eutectic solvents. J Mol Liq. 2020;298:112183. https://doi.org/10.1016/j.molliq.2019.112183.
22. Han P, Nie W, Zhao G, Gao P. Theoretical investigation on the structure and physicochemical properties of choline chloride-based deep eutectic solvents. J Mol Liq. 2022;366:120243. https://doi.org/10.1016/j.molliq.2022.120243.
23. Wu M, Liao K, Liu C, Yu G, Rahmaninia M, Li H, Li B. Integrated and sustainable preparation of functional nanocellulose via formic acid/choline chloride solvents pretreatment. Cellulose. 2021;28(15):9689–9703. https://doi.org/10.1007/s10570-021-04157-2.
24. Lynam JG, Kumar N, Wong MJ. Deep eutectic solvents' ability to solubilize lignin, cellulose, and hemicellulose; thermal stability; and density. Bioresour Technol. 2017;238:684–689. https://doi.org/10.1016/j.biortech.2017.04.079.
25. Mishra S, Pandey A, Pant K, Mishra B. Investigating the effect of mono di carboxylic acids as hydrogen bond donor on solvation of copper in choline chloride-based deep eutectic solvents. J Mol Liq. 2023;383:122142. https://doi.org/10.1016/j.molliq.2023.122142.
26. Sethi O, Singh M, Singh Kang T, Kumar Sood A. Volumetric and compressibility studies on aqueous mixtures of deep eutectic solvents based on choline chloride and carboxylic acids at different temperatures: Experimental, theoretical and computational approach. J Mol Liq. 2021;340:117212. https://doi.org/10.1016/j.molliq.2021.117212.
27. Kuddushi M, Nangala GS, Rajput S, Ijardar SP, Malek NI. Understanding the peculiar effect of water on the physicochemical properties of choline chloride based deep eutectic solvents theoretically and experimentally. J Mol Liq. 2019;278:607–615. https://doi.org/10.1016/j.molliq.2019.01.053.

28. Shekaari H, Zafarani-Moattar MT, Mokhtarpour M, Faraji S. Volumetric and compressibility properties for aqueous solutions of choline chloride based deep eutectic solvents and Prigogine–Flory–Patterson theory to correlate of excess molar volumes at T=(293.15 to 308.15). J Mol Liq. 2019;289:111077. https://doi.org/10.1016/j.molliq.2019.111077.
29. Wang Y, Ma C, Liu C, Lu X, Feng X, Ji X. Thermodynamic study of choline chloride-based deep eutectic solvents with water and methanol. J Chem Eng Data. 2020;65(5):2446–2457. https://doi.org/10.1021/acs.jced.9b01113.
30. Zuo Z, Cao B, Wang Y, Ma C, Lu X, Ji X. Thermodynamic study of choline chloride-based deep eutectic solvents with dimethyl sulfoxide and isopropanol. J Mol Liq. 2024;394:123731. https://doi.org/10.1016/j.molliq.2023.123731.
31. Haghbakhsh R, Duarte ARC, Raeissi S. Viscosity investigations on the binary systems of (1 chcl: 2 ethylene glycol) des and methanol or ethanol. Molecules. 2021;26(18):5513. https://doi.org/10.3390/molecules26185513.
32. Redlich O, Kister A. Algebraic representation of thermodynamic properties and the classification of solutions. Ind Eng Chem. 1948;40(2):345–348. https://doi.org/10.1021/ie50458a036.
33. Tahery R, Hernández A. Surface tension of binary mixtures of benzene+ propionic acid and butanoic acid between 298.15 K and 318.15 K: measurement and modeling. J Chem Thermodyn. 2022 May;168:106723. https://doi.org/10.1016/j.jct.2022.106723.
34. Mgxadeni N, Hernández A, Bahadur I, Mohammad F, Soleiman AA. Correlation and modelling the thermodynamics properties of mixtures containing zinc (II) chloride-based deep eutectic solvent and alkanols with PC-SAFT EoS, and the Nomoto's relation.". J Mol Liq. 2024;397:124155. https://doi.org/10.1016/j.molliq.2024.124155.
35. Mgxadeni N, Kabane B, Hernández A, Bahadur I, Mohammad F, Soleiman AA, Hashemi H, Kabanda MM. Application of PC-SAFT EoS and SCFT for the modeling of thermophysical properties comprising deep eutectic solvent and alcohols. Asia-Pac J Chem Eng. 2024;19(3):e3031. https://doi.org/10.1002/apj.3031.
36. Gross J, Sadowski G. Perturbed-chain SAFT: an equation of state based on a perturbation theory for chain molecules. Ind Eng Chem Res. 2001;40(4):1244–1260. https://doi.org/10.1021/ie0003887.
37. Gross J, Sadowski G. Application of the perturbed-chain SAFT equation of state to associating systems. Ind Eng Chem Res. 2002;41(22):5510–5515. https://doi.org/10.1021/ie010954d.
38. Schaaffs W. The problem of a theoretical calculation of the velocity of sound for binary liquid mixtures. Acta Acust united Ac. 1975;33:272–276. <Unfamiliar with this journal name, please check and confirm journal name>
39. Nomoto O. Empirical formula for sound velocity in liquid mixtures. J Phys Soc Jpn. 1958;13(12):1528–1532. https://doi.org/10.1143/JPSJ.13.1528.
40. Biernacki K, Souza HIK, Almeida CUM, Magalhães AL, Gonçalves MP. Physicochemical properties of choline chloride-based deep eutectic solvents with polyols: an experimental and theoretical investigation. ACS Sustain Chem& Eng. 2020;8(50):18712–18728. https://doi.org/10.1021/acssuschemeng.0c08288.
41. Ceaser R, Rosa S, Montanè D, Constantí M, Medina F. Constantí Ma, Francesc M. Optimization of softwood pretreatment by microwave-assisted deep eutectic solvents at high solids loading. Bioresour Technol. 2023;369:128470. https://doi.org/10.1016/j.biortech.2022.128470.
42. Zhang J, Yin J, Zhang Y, Zhu T, Ran H, Jiang W, Li H, Li H, Zhang M. Ming ZhangInsights into the formation mechanism of aliphatic acid-choline chloride deep eutectic solvents by theoretical and experimental research. J Mol Liq. 2022;367:120342. https://doi.org/10.1016/j.molliq.2022.120342.
43. Chen H, Wang A, Yan C, Liu S, Li L, Wu Q, Liu Y, Liu Y, Nie G, Nie S, et al. Study on the solubility of industrial lignin in choline chloride-based deep eutectic solvents. Sustainability (Basel). 2023;15(9):7118. https://doi.org/10.3390/su15097118.
44. Yu Q, Bai R, Wang F, Zhang Q, Sun Y, Zhang Y, Qin L, Wang Z, Yuan Z. A sustainable system for maleic acid synthesis from biomass-derived sugar. J Chem Technol Biotechnol. 2020;95(3):751–757. https://doi.org/10.1002/jctb.6260.
45. Jian Y, Li X, Liu Y, Chen X, Zhang Y, Baroutian S, Yu Q. Deep eutectic solvent assists H-β in aldol condensation of acetovanillone and p-hydroxybenzaldehyde to prepare a high density aviation oil precursor. Fuel. 2023;347:128491. https://doi.org/10.1016/j.fuel.2023.128491.
46. Hu S, Meng F, Huang D, Huang J, Lou W. Hydrolysis of corn stover pretreated by DESs with carbon-based solid acid catalyst. SN Appl Sci. 2020;2(7):1240. https://doi.org/10.1007/s42452-020-3022-7.
47. Chai K, Zhou Y, Lu X, Yamaguchi T, Ohara K, Liu HZF, Zhu F. Structure of choline chloride-carboxylic acid deep eutectic solvents by wide-angle X-ray scattering and DFT calculations. Phys Chem Chem Phys. 2023;25(15):10481–10494. https://doi.org/10.1039/D3CP00570D.
48. Jahan MS, Hossain S, Das SC, Rahman ML, Khan MA. Extraction and characterization of cellulose nanocrystals (CNCs) from jute fibers and other by-products towards a circular economy approach. Mater Circ Econ 2024;6:57. https://doi.org/10.1007/s42824-024-00149-2.
49. Gautam R, Kumar N, Lynam JG. Narendra Kumar, and Joan G. Lynam. Theoretical and experimental study of choline chloride-carboxylic acid deep eutectic solvents and their hydrogen bonds. J Mol Struct. 2020;1222:128849. https://doi.org/10.1016/j.molstruc.2020.128849.
50. Singh S, Aznar M, Deenadayalu N. Densities, speeds of sound, and refractive indices for binary mixtures of 1-butyl-3-methylimidazolium methyl sulphate ionic liquid with alcohols at T=(298.15, 303.15, 308.15, and 313.15). J Chem Thermodyn. 2013;57:238–247. https://doi.org/10.1016/j.jct.2012.08.030.
51. Masilo K, Bahadur I. Investigation on the molecular interaction of binary mixtures of acetophenone with carboxylic acids at various temperature: thermodynamic and spectroscopic aspects. J Chem Thermodyn. 2022;166:106667. https://doi.org/10.1016/j.jct.2021.106667.
52. Kabane B, Chokkareddy R, Redhi GG. Molecular interaction studies of binary systems comprising [C2mim] [BF4] with ethyl acetoacetate or benzaldehyde. Heliyon. 2019;5(5):e01548. https://doi.org/10.1016/j.heliyon.2019.e01548.
53. Nduli M, Deenadayalu N. Thermophysical properties of binary mixtures of (methanol or 1-ethyl-3-methylimidazolium acetate+ furfural or furfuryl alcohol) at various temperatures. J Mol Liq. 2017;241:407–421. https://doi.org/10.1016/j.molliq.2017.06.029.
54. Fortin TJ, Laesecke A, Freund M, Outcalt S. Advanced calibration, adjustment, and operation of a density and sound speed analyzer. J Chem Thermodyn. 2013;57:276–285. https://doi.org/10.1016/j.jct.2012.09.009.
55. Belhadj D, Negadi A, Hernández A, Mokbel I, Bahadur I, Negadi L. A study on mixing properties of binary mixtures of 1-hexene with alkoxyethanols at different temperatures. J Chem Thermodyn. 2022;172:106820. https://doi.org/10.1016/j.jct.2022.106820.
56. Almasi M, Hernández A. Theoretical and experimental study of triethanolamine and 1-alkanol mixtures. Fluid Phase Equilib. 2023;571:113810. https://doi.org/10.1016/j.fluid.2023.113810.
57. Ayad A, Belabbaci A, Negadi A, Hernández A, Kabane B, Bahadur I, Mohammad F, Soleiman AA, Negadi L. Measurements and modeling of thermodynamic properties of binary systems comprising (2-amino-2-methyl-1-propanol with acetonitrile, toluene, 1-pentanol or 1-hexanol) at different temperatures. J Chem Eng Data. 2023;68(11):2789–2806. https://doi.org/10.1021/acs.jced.2c00767.
58. Hernández A, Zeqiraj AZ, Aliaj FR. Densities, sound speeds, and refractive indices of 1-propanol+ cyclohexane (or cyclohexene or cyclohexanone) binary mixtures at various temperatures under atmospheric pressure: experimental and modeling study. Int J Thermophys. 2023;44(7):102. https://doi.org/10.1007/s10765-023-03211-4.
59. Almasi M, Hernández A. Experimental and theoretical studies of ethylene glycol dimethyl ether and 2-alkanol mixtures. Int J Thermophys. 2023;44(7):109. https://doi.org/10.1007/s10765-023-03221-2.
60. Almasi M, Hernández A, Zarrini J. Density and viscosity studies of ethylene glycol diethyl ether and 1-alkanol mixtures. J Chem Eng Data. 2023 Aug 10;68(8):1911–1920. https://doi.org/10.1021/acs.jced.3c00192.
61. Chabouni Y, Hernández A, Amireche F. Volumetric, optical and spectroscopic properties of binary mixtures of glycerol with butanediol isomers. Int J Thermophys. 2023;44(11):161. https://doi.org/10.1007/s10765-023-03272-5.
62. Politzer P, Murray JSJ. Mol. Mod. 2015;21:1. <The article title is missing from this reference. Please provide one. >
63. Alnefaie KA, Abu-Hamdeh NH. Specific heat and volumetric heat capacity of some saudian soils as affected by moisture and density. International conference on mechanics. Fluids. Heat. Elasticity and Electromagnetic Fields. 2013; p. 139–143.
64. Kitaigorodsky A. Molecular crystals and molecules. Elsevier; 2012.

65. Wen R, Rahn B, Magnussen OM. Potential-Dependent adlayer structure and dynamics at the ionic liquid/Au (111) interface: a molecular-scale in situ video-STM study. Angew Chem Int Ed. 2015;54(20):6062–6066. https://doi.org/10.1002/anie.201501715.
66. Jangir AK, Sethy P, Verma G, Bahadur P, Kuperkar K. An inclusive thermophysical and rheology portrayal of deep eutectic solvents (DES) for metal oxides dissolution enhancement. J Mol Liq. 2021;332:115909. https://doi.org/10.1016/j.molliq.2021.115909.
67. Shana'a M, Canfield FB. Liquid density and excess volume of light hydrocarbon mixtures at–165° C. Trans Faraday Soc. 1968;64(0):2281–2286. https://doi.org/10.1039/TF9686402281.
68. Nowosielski B, Jamrógiewicz M, Łuczak J, Warmińska D. Novel binary mixtures of alkanolamine based deep eutectic solvents with water—thermodynamic calculation and correlation of crucial physicochemical properties. Molecules. 2022;27(3):788. https://doi.org/10.3390/molecules27030788.
69. Sharma R, Jisha K, Gardas RL, Malek N, Ijardar SP. Insights into experimental and theoretical approach to physicochemical properties of aqueous PEGylated deep eutectic solvents at T=(293.15–323.15). J Mol Liq. 2022;366:120278. https://doi.org/10.1016/j.molliq.2022.120278.
70. Mokhtarpour M, Shekaari H. Measurement and correlation of thermophysical properties in aqueous solutions of some novel bio-based deep eutectic solvents (lactic acid/amino acids) at T = (298.15 to 313.15) K. J Chem Thermodyn. 2020;144:106051. https://doi.org/10.1016/j.jct.2020.106051.
71. Shekaari H, Zafarani-Moattar MT, Mohammadi B. Thermophysical characterization of aqueous deep eutectic solvent (choline chloride/urea) solutions in full ranges of concentration at T=(293.15–323.15). J Mol Liq. 2017;243:451–461. https://doi.org/10.1016/j.molliq.2017.08.051.
72. Abri A, Babajani N, Zonouz AM, Shekaari H. Spectral and thermophysical properties of some novel deep eutectic solvent based on l-menthol and their mixtures with ethanol. J Mol Liq. 2019;285:477–487. https://doi.org/10.1016/j.molliq.2019.04.001.
73. Handa YP, Benson GC. Volume changes on mixing two liquids: A review of the experimental techniques and the literature data. Fluid Phase Equilib. 1979;3(2–3):185–249. https://doi.org/10.1016/0378-3812(79)85010-4.
74. Kim KS, Park BH. olumetric properties of solutions of choline chloride+ glycerol deep eutectic solvent with water, methanol, ethanol, or iso-propanol. J Mol Liq. 2018;254:272–279. https://doi.org/10.1016/j.molliq.2018.01.087.
75. Haghbakhsh R, Raeissi S. A study of non-ideal mixtures of ethanol and the (1 choline chloride+ 2 ethylene glycol) deep eutectic solvent for their volumetric behaviour. J Chem Thermodyn. 2020;150:106219. https://doi.org/10.1016/j.jct.2020.106219.
76. Haghbakhsh R, Raeissi S. Experimental investigation on the volumetric properties of mixtures of the deep eutectic solvent of Ethaline and methanol in the temperature range of 283.15 to 323.15 K. J Chem Thermodyn. 2020;147:106124. https://doi.org/10.1016/j.jct.2020.106124.
77. Piehl J, Samimi-Abianeh O. Measuring the adiabatic ignition delay of n-pentane mixture using rapid compression machine. J Therm Sci. 2020;1–9.
78. Gowrisankar M, Sivarambabu S, Venkateswarlu P, Kumar KS. Excess volumes, speeds of sound, isentropic compressibilities and viscosities of binary mixtures of N-ethyl aniline with some aromatic ketones at 303.15 K. Bull Korean Chem Soc. 2012;33(5):1686–1692. https://doi.org/10.5012/bkcs.2012.33.5.1686.
79. Nabi A, Md Zain SB, Jesudason CG. Densities, ultrasonic speeds, refractive indices, and COSMO analysis for binary mixtures of dichloromethane with acetone and dimethylsulfoxide at T=(298.15, 303.15, and 308.15). Chem Eng Commun. 2018;205(4):479–491. https://doi.org/10.1080/00986445.2017.1403908.
80. Begum Z, Sandhya Sri PB, Karuna Kumar DB, Rambabu C. Thermodynamic, ultrasonic and FT-IR studies on binary liquid mixtures of anisaldehyde and alkoxyethanols at different temperatures. J Mol Liq. 2013;178:99–112. https://doi.org/10.1016/j.molliq.2012.11.016.
81. Roy MN, Sinha A, Sinha B. Excess molar volumes, viscosity deviations and isentropic compressibility of binary mixtures containing 1, 3-dioxolane and monoalcohols at 303.15 K. J. J Solution Chem. 2005;34(11):1311–1325. https://doi.org/10.1007/s10953-005-8022-0.
82. Pal A, Kumar H, Kumar A. Speeds of sound, excess isentropic compressibility and apparent molar compressibility properties for binary mixtures of dipropylene glycol tert.-butyl ether with methanol, 1-propanol, 1-pentanol and 1-heptanol at 298.15 K. Z Phys Chem. 2007;221(6):757–773. https://doi.org/10.1524/zpch.2007.221.6.757.
83. Pandey JD, Kumar V, Saxena M. Evaluation of Jacobson's constant and intermolecular free-length as a function of pressure and temperature for cryogenic liquids. Ultrasonics. 1979;17(4):153–158. https://doi.org/10.1016/0041-624X(79)90032-5.
84. Pandey J, Dey R, Chhabra J. Thermoacoustical approach to the intermolecular free-length of liquid mixtures. PhysChemComm. 2003;6(14):55. https://doi.org/10.1039/b307435h.
85. Singh D, Gardas RL. Influence of N-1 alkyl substituent on apparent molar properties of 1, 2, 4-triazolium based ionic liquids in aqueous solutions. J Mol Liq. 2018;250:477–484. https://doi.org/10.1016/j.molliq.2017.12.024.
86. Grande MdelC, Juliá JÁ, Barrero CR, Marschoff CM. Sound velocity measurements in the water + acetonitrile system at temperatures from 293.15 to 323.15 K and its implications on thermodynamic data processing. Phys Chem Liq. 2013:51(4):457–468. https://doi.org/10.1080/00319104.2012.737790.
87. Zaoui-Djelloul-Daouadji M, Mokbel I, Bahadur I, Negadi A, Jose J, Ramjugernath D, Ebenso EE, Negadi L. Vapor-liquid equilibria, density and sound velocity measurements of (water or methanol or ethanol + 1,3-propanediol) binary systems at different temperatures. Thermochim Acta. 2016 Oct;642:111–123. https://doi.org/10.1016/j.tca.2016.09.005.
88. Anwar N, Riyazuddeen, Yasmeen S. Volumetric, compressibility and viscosity studies of binary mixtures of [EMIM][NTf2] with thylacetate/methanol at (298.15–323.15). J Mol Liq. 2016;224:189–200. https://doi.org/10.1016/j.molliq.2016.09.077.
89. Benkelfat-Seladji NL, Ouaar F, Hernández A, Bahadur I, Muñoz-Rujas N, Kumar Singh S, Montero E, Chiali-Baba Ahmed N, Negadi L. Density, speed of sound, refractive index of binary mixtures containing 2-ethoxyethanol and some alcohols: measurement and correlation. J Chem Thermodyn. 2022;170:106762. https://doi.org/10.1016/j.jct.2022.106762.
90. Bahadur I, Deenadayalu N, Ramjugernath D. Effects of temperature and concentration on interactions in methanol+ ethyl acetate and ethanol+ methyl acetate or ethyl acetate systems: insights from apparent molar volume and apparent molar isentropic compressibility study. Thermochim Acta. 2014;577:87–94. https://doi.org/10.1016/j.tca.2013.12.016.
91. Sun T, Biswas SN, Trappeniers NJ, Ten Seldam CA. Acoustic and thermodynamic properties of methanol from 273 to 333 K and at pressures to 280 MPa. J Chem Eng Data. 1988;33(4):395–398. https://doi.org/10.1021/je00054a002.